

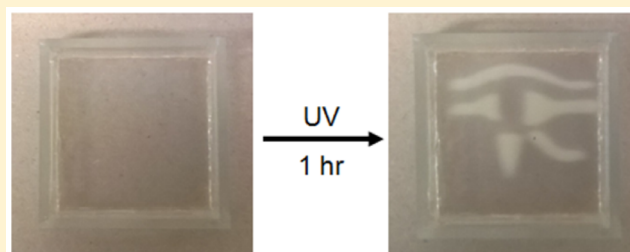
Photopatterned Multidomain Gels: Multi-Component Self-Assembled Hydrogels Based on Partially Self-Sorting 1,3:2,4-Dibenzylidene-D-sorbitol Derivatives

Daniel J. Cornwell, Oliver J. Daubney, and David K. Smith*

Department of Chemistry, University of York, Heslington, York YO10 SDD, U.K.

S Supporting Information

ABSTRACT: We report a multicomponent self-assembling system based on 1,3:2,4-dibenzylidene-D-sorbitol (DBS) derivatives which form gels as the pH is lowered in a controlled way. The two DBS gelators are functionalized with carboxylic acids: the first in the 4-position of the aromatic rings (DBS-CO₂H), the second having glycine connected through an amide bond and displaying a terminal carboxylic acid (DBS-Gly). Importantly, these two self-assembling DBS-acids have different pK_a values, and as such, their self-assembly is triggered at different pHs. Slowly lowering the pH of a mixture of gelators using glucono- δ -lactone (GdL) initially triggers assembly of DBS-CO₂H, followed by DBS-Gly; a good degree of kinetic self-sorting is achieved. Gel formation can also be triggered in the presence of diphenyliodonium nitrate (DPIN) as a photoacid under UV irradiation. Two-step acidification of a mixture of gelators using (a) GdL and (b) DPIN assembles the two networks sequentially. By combining this approach with a mask during step b, multidomain gels are formed, in which the network based on DBS-Gly is positively patterned into a pre-existing network based on DBS-CO₂H. This innovative approach yields spatially resolved multidomain multicomponent gels based on programmable low-molecular-weight gelators, with one network being positively “written” into another.



INTRODUCTION

The self-assembly of supramolecular gels is a simple, effective way of creating nanostructured soft materials with wide-ranging applications.¹ Molecular-scale information programmed into low-molecular-weight gelators by organic synthesis is translated up to the nanoscale through noncovalent interactions which underpin the formation of a sample-spanning network, usually comprised of self-assembled nanofibers.² In recent times, there has been increasing interest in the assembly of multicomponent gels with the potential for each individual component to endow the gel with a different behavior.³ Well-designed gelators are capable of self-sorting, with each gelator preferentially assembling into its own nanoscale network, often driven by structural differences between them.⁴ In key work, Adams and co-workers demonstrated that gelators with different pK_a values could be assembled sequentially, with controlled protonation driving the self-assembly of each network in turn, an elegant approach to kinetically controlled self-sorting.⁵

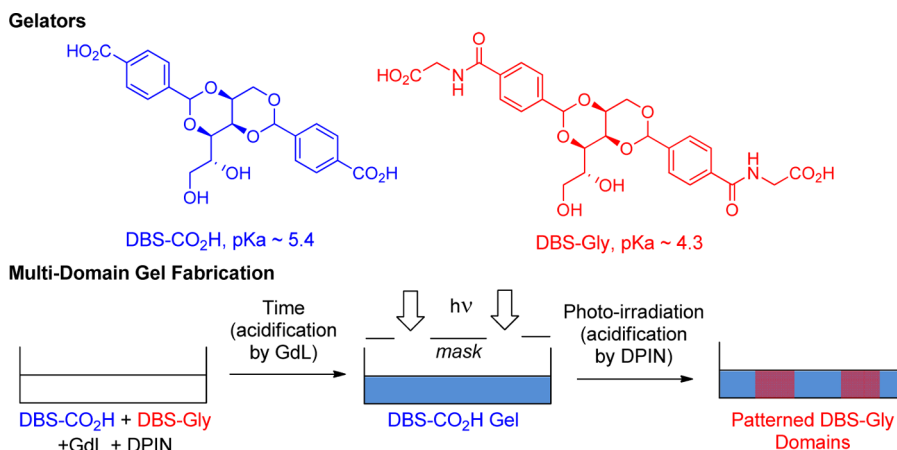
A significant drawback of self-assembled gels is the difficulty of achieving morphological structuring on a macroscopic scale, i.e., spatial control. Supramolecular gels usually self-assemble from the solution phase using a heat-cool cycle, or bulk treatment of a sample with an activating reagent. As such, most gels simply form within the container in which they are made. It is desirable to achieve a greater degree of spatial control over gel-formation, as this would allow the creation of morphologies that may be able to participate more intelligently in high-tech

applications—from conducting soft materials to tissue engineering.² With this goal in mind, we recently photopatterned a polymer gel within a self-assembled gel using photopolymerization and a mask,⁶ leading to what we defined as a “multidomain gel”. Those regions based only on the supramolecular gel were soft and deformable, whereas those which also included the cross-linked polymer gel network were robust. Photoactivation of gelation is clearly a powerful strategy by which spatial control can be achieved, and is widely used in polymer gels.⁷ However, photoactivation of low-molecular-weight gelation is relatively rare. There are a number of reports in which gels can be photoswitched between gel and sol, although this has mainly only been performed on bulk samples.⁸ Of particular relevance, the research groups of Adams and van Esch have reported the use of a photoacid as a proton source to trigger the formation of simple gels on exposure to UV, with a degree of spatial patterning.⁹ Spatial resolution has also been previously achieved within a multicomponent low-molecular-weight gel (LMWG) using an electrochemical method,¹⁰ but this requires electrode insertion, disturbing the sample. Photopatterning of a multicomponent gel has very recently been reported using a “negative etching” approach: two networks were assembled together, and one was then subsequently disassembled by irradiation.¹¹

Received: September 15, 2015

Published: December 8, 2015

Scheme 1. Gelators Investigated in This Paper and the Fabrication Approach to Multidomain Gels, in which Glucono- δ -Lactone (GdL) is Used to Slowly (and Preferentially) Form the DBS-CO₂H Gel Network Owing to the Higher pK_a of this Gelator, and Photoactivation of Diphenyl Iodonium Nitrate (DPIN) under a Mask Subsequently Patterns DBS-Gly Domains into It



In contrast to previous studies, our approach here is different, leading to “positive writing”, in which the second network is activated and assembled in the presence of the first only in those regions irradiated (Scheme 1). We reasoned that positive photopatterning of one gel within another, in addition to having advantages over negative etching,¹¹ also improves on simple patterning of a single gel in solvent,⁹ as the supporting preformed gel matrix will limit convection and diffusion effects, hence enhancing spatial resolution.

Our group has recently been working on gelators based on the versatile 1,3:2,4-dibenzylidene-D-sorbitol (DBS) framework. DBS and derivatives are considered to have low toxicity, and their gels are currently used in applications ranging from personal care products to plastic clarification.¹² To expand the scope of DBS-based gelators away from organic media, we have recently developed derivatives with the aromatic “wings” modified by carboxylic acid¹³ (DBS-CO₂H) or acyl hydrazide¹⁴ (DBS-CONHNH₂) functional groups—giving true hydrogelators. For this study, we further modified DBS-CO₂H to yield a hydrogelator with a different pK_a value, capable of kinetic self-sorting, and hence able to be individually addressed in a stepwise manner using a photoacid and enabling photopatterning (Scheme 1).

RESULTS AND DISCUSSION

Synthesis and Characterization of DBS-Gly. We coupled methyl-ester-protected glycine to DBS-CO₂H using *O*-(benzotriazol-1-yl)-*N,N,N',N'*-tetramethyluronium tetrafluoroborate (TBTU) in the presence of diisopropylethylamine (DIPEA) to yield 1,3:2,4-dibenzylidene-D-sorbitol-dicarbonyl-glycine methyl ester in 67% yield. Subsequent hydrolysis of the methyl ester groups with 2 equiv of aqueous NaOH (1 M), provided 1,3:2,4-dibenzylidene-D-sorbitol-dicarbonyl-glycine (DBS-Gly) in 65% yield (see Supporting Information for full details). Although DBS derivatives are widely investigated and industrially applied, with many patents in place,¹² this is the first reported example incorporating an amino acid.

As expected, DBS-Gly formed gels by basification (to deprotonate and dissolve the gelator) followed by slow acidification (to reprotonate, lowering solubility and encouraging self-assembly).¹⁵ We employed glucono- δ -lactone (GdL), in known amounts of ≥ 10 mg mL⁻¹ as acidification agent; GdL hydrolysis slowly acidifies the solution and is well-known to

give homogeneous gels.^{15c} Samples were left overnight and translucent gels were observed (Figure S1). The minimum gelation concentration (MGC) was 0.45% wt/vol (8.03 mM), with a T_{gel} value of ca. 67 °C (corresponding to gel collapse).

Gelation kinetics were monitored using NMR methods¹⁶ to follow the assembly of DBS-Gly after the addition of GdL. NMR allows (with reference to a “mobile” internal standard, DMSO) quantification of the concentration of gelator present in the mobile phase, and by inference, how much has assembled in the “solid-like” fibers.^{5a,6,13} From Figure 1a, it is clear that there is some initial rapid assembly, as the concentration of mobile gelator drops from ca. 8 to ca. 7 mM in the first 30 min. This may be attributed to a “burst” release of protons as GdL is quickly converted to gluconic acid by residual NaOH; in situ monitoring of pH indicated a rapid drop from ca. 10.5 to ca. 6.8

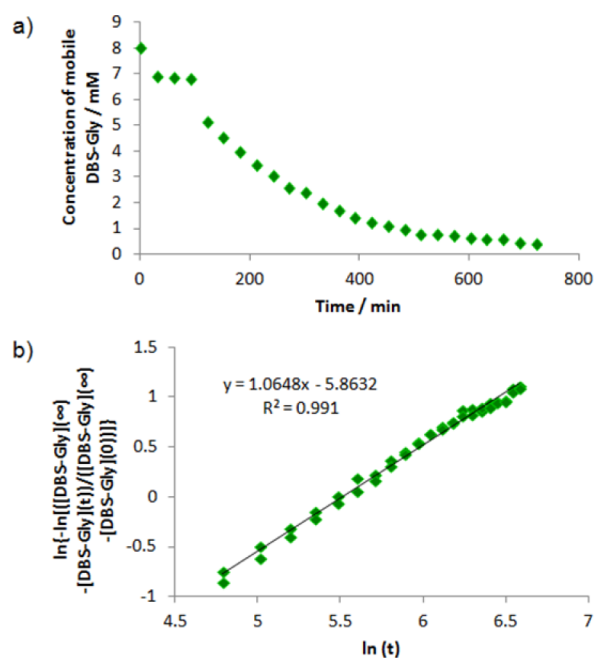


Figure 1. (a) Kinetics of formation of DBS-Gly network as monitored by NMR spectroscopy; (b) Avrami plot for DBS-Gly network formation, where the Avrami exponent, n , is equivalent to the gradient of line of best fit.

immediately after the addition of GdL (see Figure S3). There is then a period of buffering, presumably as the pH gradually lowers further toward the pK_a value of DBS-Gly; once this value is reached, there is slow assembly of the LMWG network over the course of several hours. The data were fitted to Avrami's kinetic model (Figure 1b, see SI for full details of method).^{17,18} For DBS-Gly, the value of the Avrami exponent, n , was found to be 1.06 (Figure 1b), indicative of the formation of one-dimensional nanofibers with relatively little branching.

The minimum amount of GdL required to form gels from DBS-Gly (ca. 10 mg mL⁻¹) was significantly higher than that for DBS-CO₂H (ca. 6 mg mL⁻¹ by the same method). We determined the pK_a value by titration against HCl; its self-assembly into gel nanofibers around the pK_a value means that these values can only be estimated.¹⁹ The pK_a value for DBS-Gly was ca. 4.3 (Figure S5), but the pK_a value determined for DBS-CO₂H was ca. 5.4 (Figure S6). Rationalizing this difference is challenging, as apparent pK_a values of gelators are affected by the self-assembly step, which can perturb the protonation equilibrium, changing the pK_a from what might be expected for small molecule analogues.²⁰ It should also be noted that these gelators each have two acids, which could have distinct pK_a values. However, these acids are relatively distant from one another and the gelator is relatively rigid; as such we only observe one apparent pK_a . The final pH of these gels is ca. 4.0, and we do not see any evidence of acid-mediated acetal hydrolysis. In summary, and most importantly, the structural change programmed into the gelator by organic synthesis has a direct impact on the pK_a , and hence the pH at which network assembly is initiated.

Multi-Component Self-Assembly and Self-Sorting of DBS-CO₂H and DBS-Gly. Because of their significant differences in pK_a values, we reasoned that kinetically controlled self-sorting of DBS-Gly and DBS-CO₂H may occur. Indeed, a sample containing 0.45 wt %/vol DBS-CO₂H (10.08 mM), 0.45 wt %/vol DBS-Gly (8.03 mM), and 18 mg mL⁻¹ of GdL yielded a translucent gel (Figure S2), indicating that a combination of the two gelators could indeed form a gel.

We used NMR to follow the assembly of gelators into the solid-like nanofibers of the gel network. Solutions were prepared containing 0.45 wt %/vol of both gelators, in D₂O (with DMSO internal standard), the minimum amount of NaOH_(aq) (0.5 M) to dissolve them, and varying amounts of GdL: (a) 4 mg mL⁻¹ (22.5 mM), (b) 5.7 mg mL⁻¹ (32.0 mM), and (c) 14.3 mg mL⁻¹ (80.3 mM). The concentration of the mobile components was determined from the spectra, and from this the percent of gelator assembled into a network was inferred. We reasoned that the protons released from hydrolysis would initially protonate DBS-CO₂H in preference to DBS-Gly leading to kinetic control over self-sorting.

On increasing the amount of GdL (Figure 2a–c), an increased percentage of both gelators was assembled. Assembly of DBS-CO₂H is indeed initially favored (Figure 2a). With more GdL (Figure 2b), ca. 90% of DBS-CO₂H assembles, but only ca. 20% of DBS-Gly. It should be noted that there is an initial rapid assembly of both gelators, possibly attributed to the initial rapid pH drop (Figure S3). When using a large excess of GdL (Figure 2c), continuous gradual assembly of DBS-CO₂H up to ca. 300 min was observed, at which point 100% of the gelator was incorporated into the solid-like network. Up to this point, only ca. 20% of DBS-Gly was immobilized. After this point (ca. 400 min), the DBS-Gly initiates rapid assembly, as

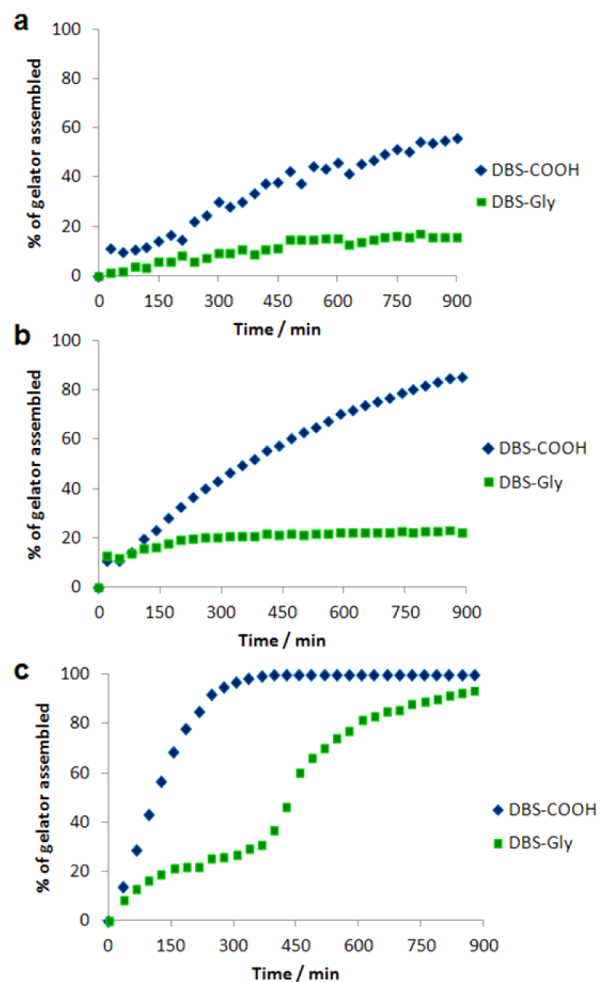


Figure 2. Percentage of gelator assembled into a network for multicomponent systems of DBS-CO₂H (10.08 mM) and DBS-Gly (8.03 mM), with (a) 22.5 mM, (b) 32.0 mM, and (c) 80.3 mM GdL as the only proton source, added in one batch.

the pH drops to the pK_a value of this LMWG and triggers its assembly. By the end of the experiment, over 90% of DBS-Gly had also been immobilized. Hence, there is a good degree of stepwise kinetic control.

We then examined the nanostructure of each of these gels using scanning electron microscopy (SEM, Figure S9). Samples were prepared by freeze-drying in liquid nitrogen, followed by lyophilizing overnight, minimizing thermal reorganization, and allowing us to visualize the relatively “expanded” structure of the overall network, which had not collapsed on drying. The nanofibers are fairly similar in each case, suggesting that the two gelators do not inhibit one another's self-assembly.

Rheological analysis was then performed (Table 1). The strongest gel as characterized by its G' value was DBS-CO₂H (4060 Pa); DBS-Gly was significantly weaker (1140 Pa). The

Table 1. Rheological Performance of Individual Gelators and Multi-Component System^a

LMWG	G' /Pa	G'' /Pa
DBS-CO ₂ H, 0.45 wt %/vol	4060	373
DBS-Gly, 0.45 wt %/vol	1140	80
DBS-CO ₂ H/DBS-Gly, both 0.45 wt %/vol	2040	149

^aShear strain = 0.3%, frequency = 1 Hz.

mixed two-component gel was somewhat intermediate between the two in terms of rheological performance ($G' = 2040$ Pa), suggesting that the fibers of DBS-Gly in the two-component gel may prevent DBS-CO₂H from forming its most optimal sample-spanning network. Similar effects are often observed when mixing self-assembled gels with polymers, the presence of which can somewhat disrupt the formation of a sample-spanning network.²¹

Dual Activation: Combination of GdL with Photoactivation. In light of this system's two-step activation mechanism (Figure 2c), we reasoned that it may be possible to use two different proton sources, with one being used to activate each of the networks. Although Adams and co-workers have previously explored two-step acidification, they did this within a single-component gel.²² Ideally, our second source of protons should have an orthogonal control mechanism. We decided to employ the photoacid generator (PAG) diphenyliodonium nitrate (DPIN). On exposure to UV light in the presence of water, DPIN is hydrolyzed, generating nitric acid as one of the products. We measured λ_{max} to be 287 nm (Figure S10), and used a high-intensity UV lamp with $\lambda \approx 300\text{--}400$ nm (overlapping with DPIN's absorbance) for activation. Although the use of a PAG has previously been shown to make individual pH-sensitive gelation systems light-responsive,⁹ our approach is significantly different as we photopattern one gel within another. We hoped to first observe mostly formation of the DBS-CO₂H network via GdL hydrolysis/activation; then with activation of DPIN by UV light the assembly of the second network based on DBS-Gly to form the dual-network gel from this second source of protons (Scheme 1). With $\text{p}K_{\text{a}}$ values for gluconic acid (produced by GdL) and nitric acid (produced by DPIN) of 3.86 and -1.4 , respectively, these acidification agents are well chosen for the stepwise protonation of DBS-CO₂H and DBS-Gly, which have $\text{p}K_{\text{a}}$ values of 5.4 and 4.3, respectively.

Initially, we characterized the ability of DPIN to photoactivate formation of a simple, single-component gel from DBS-Gly. Solutions of 0.45% wt/vol DBS-Gly with varying amounts of DPIN in NMR tubes were cured under UV light for 30 min to produce opaque gels (we attribute the opaqueness to the formation of insoluble iodobenzene as a byproduct of photoirradiation). The optimal amount of DPIN was 8 mg mL⁻¹ (ca. 3 equiv), which we reason is sufficient to suitably acidify the solution to below the $\text{p}K_{\text{a}}$ of DBS-Gly. We also noted that the initial addition of a small amount of HCl improved the level of reprotonation of DBS-Gly, presumably as this helped neutralize any excess NaOH prior to photoacid activation.

We then used NMR methods to follow the kinetics of DBS-Gly assembly into solid-like nanostructures on photoactivation (Figure S12). Self-assembly occurred much more rapidly: ca. 1 h using DPIN, compared to ca. 11 h with GdL (due to faster generation of protons). The Avrami exponent, $n = 1.08$, was similar to that when GdL was used ($n = 1.06$), indicating that DBS-Gly still assembles into mostly 1D nanostructures with little branching.

We then attempted to make gels of DBS-Gly in 2.5-mL sample vials using a 1 mL solution of 0.45% wt/vol DBS-Gly with 8 mg mL⁻¹ DPIN. However, we found that we could only produce opaque suspensions of partial gels (Figure S13); using smaller volumes produced similar results, even with extended UV exposure and water cooling to prevent UV-induced heating effects, and solvent evaporation, from disrupting gelation. On the other hand, using a 5 cm \times 5 cm dish instead of vials as the

container for 5 mL of a similarly prepared solution resulted in the formation of a weak, opaque gel (Figure S14). We therefore reasoned that photoactivation using DPIN was most effective in samples and containers which were relatively shallow, so that effective penetration of the UV light could be achieved, yielding homogeneous dispersion of DBS-Gly nanofibers. As such, we did not form gels in sample vials (as is often the case in gelation studies) with DPIN and instead made them in tray-molds. The sample-spanning gels formed in the trays were relatively weak, and difficult to study using rheology. In addition to the impact of different sample dimensions in tray-molds, it should also be noted that Adams and co-workers have recently reported that the mechanical properties of acid-functionalized hydrogels depend on the kinetics of acidification.²³ Given DPIN activates our system in <1 h, whereas GdL takes ca. 11 h, it is therefore not surprising that there are some mechanical differences dependent on the mode of activation.

We next studied the activation of the multicomponent system with a two-step acidification procedure using NMR analysis. We used 32.0 mM GdL, as previous analysis by ¹H NMR (in the absence of DPIN) showed that this resulted in ca. 90% DBS-CO₂H and only ca. 20% DBS-Gly assembling into solid-like nanostructures (Figure 2b). We also introduced DPIN at a concentration of 23.3 mM. Unfortunately, the presence of aromatic signals from DPIN in the NMR spectrum made it somewhat difficult to accurately quantify how much of each gelator was incorporated into the network at any given time, due to some overlap between signals. However, the disappearance of the signals could still be qualitatively observed (Figure 3). After standing overnight, the resonances associated with DBS-CO₂H were significantly reduced compared to those for DBS-Gly as a result of activation by GdL. The NMR tube was then exposed to high-intensity UV light for 30 min, after which the sample became visibly more opaque; this change was not observed in the absence of DPIN. The signals

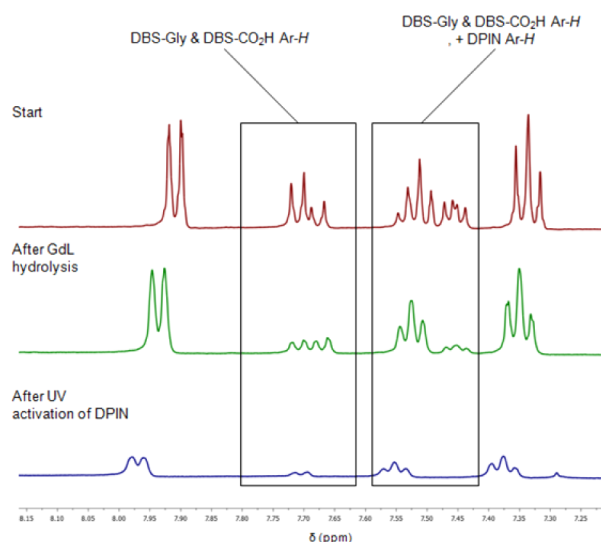


Figure 3. ¹H NMR spectra (aromatic region) for multicomponent gel of DBS-Gly (0.45 wt %/vol) and DBS-CO₂H (0.45 wt %/vol) incorporating both GdL (32.0 mM) and DPIN (23.3 mM) as proton sources. Spectra were recorded after initial preparation of the solution (top), after GdL hydrolysis (center), and after UV activation of DPIN (bottom). The highlighted peaks decrease in intensity after each proton source has been activated, showing incorporation into the solid-like network of (i) DBS-CO₂H and (ii) DBS-Gly.

corresponding to both LMWGs had decreased further: those for DBS-Gly decreased very significantly indeed and the small amount of remaining DBS-CO₂H had also disappeared. As such, the NMR experiment supports the view that in step (i), GdL primarily activates DBS-CO₂H, and in step (ii) DPIN primarily activates DBS-Gly, with the two nanoscale networks being formed in the two individual steps. Furthermore, this study demonstrates that 30 min of photoradiation is sufficient for photoinitiated gelation to be complete, indicating that there are no problems with slow kinetics in this system, unlike some other examples of photoactivated gels.

We examined these multicomponent systems on the nano/micro scale by SEM, both before and after UV activation of the PAG (Figure S15). The networks are reasonably similar in appearance to those formed when only GdL was used as a proton source, which would support the view that GdL/DPIN is an effective two-step approach for activating this system.

Photopatterning: Spatial Control over Self-Assembly Using Dual Activation Methodology. Finally, and most importantly, we investigated the possibility of photopatterning these multicomponent systems using the two different activators to achieve spatial control. We reasoned that the rapid kinetics of the photoinduced gelation combined with the assembly of DBS-Gly within a preformed gel of DBS-CO₂H, hence preventing convection and diffusion effects,²⁴ could potentially lead to spatial resolution and precise control over the formation of multidomain gels.

To form such spatially resolved gels, a solution (5 mL) of both gelators at 0.45 wt %/vol, plus GdL (32.0 mM) and DPIN (23.3 mM), was poured into a mold (5 cm × 5 cm × 0.5 cm). The solution was left overnight to allow GdL hydrolysis to take place. The next day, a translucent gel had formed. The NMR study described above, and the physical appearance of the gel, would support the view that the solid-like network of this material consisted mostly of a DBS-CO₂H network, with some (ca. 20%) DBS-Gly. A mask was then placed over the top of the mold, and the gel was exposed to UV light for 1 h, enough time to complete photoinitiated gelation as indicated by the previous NMR study. The mold was cooled in a water bath to prevent UV-induced heating effects from disrupting gelation. After photoradiation, an opaque, well-resolved pattern was formed within the gel (Figure 4), indicating that only in those regions exposed to UV light through the mask was the PAG activated.

To ensure that the protons generated by activation of the PAG only activated DBS-Gly in the patterned region, and did not diffuse out to cause DBS-Gly network formation outside of

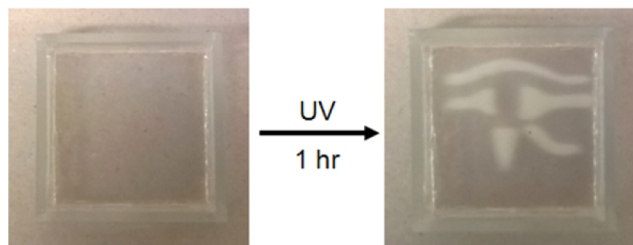


Figure 4. Photopatterning of multicomponent gel of DBS-CO₂H + DBS-Gly in a mold (dimensions 5 cm × 5 cm). After formation of translucent gel using hydrolysis of GdL as proton source (left), exposure to UV through a photomask activates DPIN only in exposed regions, leading to positive writing of a photopatterned second network in some areas, visualized by the gel changing from translucent to opaque as the second network forms (right).

the patterned domain, we used Congo Red as a pH indicator. For this experiment, a photopatterned gel was prepared in which one-half of the material was exposed to UV light during curing, and the other half was masked. After curing, the indicator was then applied in small portions across the gel to determine the pH in each of the two domains. Pleasingly, we observed that in the domain where DPIN was not activated, the indicator remained bright red, indicating a pH above ca. 5, whereas in the domain where DPIN had been activated the indicator became red–purple, indicating a pH of ca. 4 (Figure 5). Even after several hours, the colors did not appear to

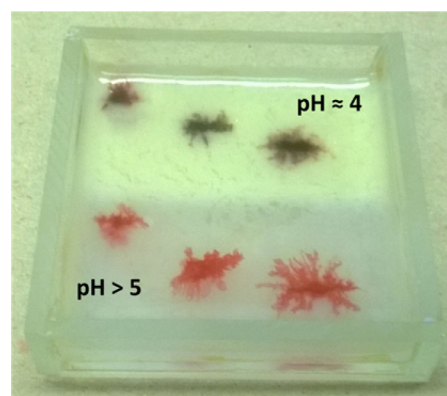


Figure 5. Photopatterned multicomponent gel of DBS-CO₂H + DBS-Gly in which one-half has been exposed to UV to activate DPIN (upper, opaque half) while one-half was left unexposed (lower, translucent half). Congo Red indicator has been applied, showing that pH > 5 in the unexposed region, and pH ≈ 4 in the photopatterned region, indicating that the protons generated during DPIN activation remain in the patterned region.

change, suggesting that in regions where DPIN is activated, the protons generated do not diffuse out, even after some time. This is supportive of the view that the protons are associated with the self-assembled, solid-like DBS-Gly network, limiting their diffusion. As such, this study confirms that DPIN-induced network formation only occurs within the photoexposed regions.

This demonstrates highly controllable assembly of a second component in the presence of a preassembled first component using photoinitiation. In this way, one gel network can be “positively” written into another, in contrast to a recent study using “negative etching” where one gel network was removed from a dual network system.¹¹ Importantly, the kinetics are sufficiently fast for the patterns generated to have good levels of resolution. As such, we propose this as an effective general route to patterning multidomain low-molecular-weight gels.

CONCLUSIONS

In summary, novel amino acid functionalized DBS-derivative, DBS-Gly, has a pK_a value significantly different from that of our standard carboxylic acid functionalized DBS-CO₂H, enabling these two gelators to undergo partial kinetic self-sorting.

Combining two different activation methods: (i) GdL and (ii) a photoacid DPIN, then allowed us to (i) mainly activate DBS-CO₂H, and (ii) photochemically activate mainly DBS-Gly. Performing the second step of this dual-activation process through a mask allowed us to positively photopattern one low-molecular-weight gel network (DBS-Gly) into another (DBS-CO₂H), and hence obtain a largely self-sorted multidomain

material with spatial resolution. This constitutes a very rare example of a multidomain supramolecular gel, and the first with positive photopatterning.

These systems have considerable potential for future development. There is huge scope for morphological design using this approach, limited only by the possibilities of photoactivation. There is also potential to synthesize DBS derivatives functionalized with other amino acids/peptides, opening this class of industrial material to a wide range of biomedical applications. Furthermore, our photoactivated approach to gelation described here could be very simply combined with other hydrogels. Such materials could be viable for controlled release or tissue engineering applications. Two-photon methods could give rise to truly three-dimensional multidomain supramolecular gel architectures. Work toward these goals is in progress within our laboratory. The highly responsive and programmable nature of supramolecular gels provides these materials with new horizons compared with the very widely investigated photopatterned polymer gels; as such, we believe their future is bright.

■ ASSOCIATED CONTENT

● Supporting Information

The Supporting Information is available free of charge on the ACS Publications website at DOI: 10.1021/jacs.5b09691.

Synthesis and characterization of DBS-Gly, preparation procedures for gels and solutions, Avrami equation, NMR data, titration plots, rheological data, and SEM images (PDF)

■ AUTHOR INFORMATION

Corresponding Author

*david.smith@york.ac.uk

Notes

The authors declare no competing financial interest.

■ ACKNOWLEDGMENTS

D.J.C. thanks University of York for funding via a Teaching Studentship. We thank Meg Stark, Technology Facility, Department of Biology, University of York, for her assistance with SEM imaging. We thank reviewers for prompting us to carry out the experiment in Figure 5, which significantly strengthened the analysis of our data.

■ REFERENCES

- (1) (a) Sangeetha, N. M.; Maitra, U. *Chem. Soc. Rev.* **2005**, *34*, 821–836. (b) Hirst, A. R.; Escuder, B.; Miravet, J. F.; Smith, D. K. *Angew. Chem., Int. Ed.* **2008**, *47*, 8002–8018. (c) Banerjee, S.; Das, R. K.; Maitra, U. *J. Mater. Chem.* **2009**, *19*, 6649–6687. (d) Skilling, K. J.; Citossi, F.; Bradshaw, T. D.; Ashford, M.; Kellam, B.; Marlow, M. *Soft Matter* **2014**, *10*, 237–256.
- (2) (a) Weiss, R. G., Terech, P., Eds. *Molecular Gels: Materials with Self-Assembled Fibrillar Networks*; Springer: Dordrecht, Netherlands, 2006. (b) Estroff, L. A.; Hamilton, A. D. *Chem. Rev.* **2004**, *104*, 1201–1218. (c) Steed, J. W. *Chem. Commun.* **2011**, *47*, 1379–1383. (d) Escuder, B.; Miravet, J. G. eds. *Functional Molecular Gels*; Royal Society of Chemistry, Cambridge, 2014; (e) Weiss, R. G. *J. Am. Chem. Soc.* **2014**, *136*, 7519–7530.
- (3) (a) Buerkle, L. E.; Rowan, S. J. *Chem. Soc. Rev.* **2012**, *41*, 6089–6102. (b) Raeburn, J.; Adams, D. J. *Chem. Commun.* **2015**, *51*, 5170–5180.
- (4) (a) Messmore, B. W.; Sukerkar, P. A.; Stupp, S. I. *J. Am. Chem. Soc.* **2005**, *127*, 7992–7993. (b) Hirst, A. R.; Huang, B.; Castelletto,

- V.; Hamley, I. W.; Smith, D. K. *Chem. - Eur. J.* **2007**, *13*, 2180–2188. (c) Sugiyasu, K.; Kawano, S. I.; Fujita, N.; Shinkai, S. *Chem. Mater.* **2008**, *20*, 2863–2865. (d) Moffat, J. R.; Smith, D. K. *Chem. Commun.* **2009**, 316–318. (e) Moffat, J. R.; Coates, I. A.; Leng, F. J.; Smith, D. K. *Langmuir* **2009**, *25*, 8786–8793. (f) Cicchi, S.; Ghini, G.; Lascialfari, L.; Brandi, A.; Betti, F.; Berti, D.; Baglioni, P.; Di Bari, L.; Pescitelli, G.; Mannini, M.; Caneschi, A. *Soft Matter* **2010**, *6*, 1655–1661. (g) Smith, M. M.; Smith, D. K. *Soft Matter* **2011**, *7*, 4856–4860. (h) Das, A.; Ghosh, S. *Chem. Commun.* **2011**, *47*, 8922–8924. (i) Velazquez, D. G.; Luque, R. *Chem. - Eur. J.* **2011**, *17*, 3847–3849. (j) Adhikari, B.; Nanda, J.; Banerjee, A. *Soft Matter* **2011**, *7*, 8913–8922. (k) Smith, M. M.; Edwards, W.; Smith, D. K. *Chem. Sci.* **2013**, *4*, 671–676. (l) Tena-Solsona, M.; Escuder, B.; Miravet, J. F.; Castelletto, V.; Hamley, I. W.; Dehsorkhi, A. *Chem. Mater.* **2015**, *27*, 3358–3365.
- (5) (a) Morris, K. L.; Chen, L.; Raeburn, J.; Sellick, O. R.; Cotanda, P.; Paul, A.; Griffiths, P. C.; King, S. M.; O'Reilly, R. K.; Serpell, L. C.; Adams, D. J. *Nat. Commun.* **2013**, *4*, 1480. (b) Colquhoun, C.; Draper, E. R.; Eden, E. G. B.; Cattoz, B. N.; Morris, K. L.; Chen, L.; McDonald, T. O.; Terry, A. E.; Griffiths, P. C.; Serpell, L. C.; Adams, D. J. *Nanoscale* **2014**, *6*, 13719–13725.
- (6) Cornwell, D. J.; Okesola, B. O.; Smith, D. K. *Angew. Chem., Int. Ed.* **2014**, *53*, 12461–12465.
- (7) (a) Luo, Y.; Shoichet, M. S. *Nat. Mater.* **2004**, *3*, 249–253. (b) Luo, Y.; Shoichet, M. S. *Biomacromolecules* **2004**, *5*, 2315–2323. (c) Hahn, M.; Miller, J.; West, J. *Adv. Mater.* **2006**, *18*, 2679–2684. (d) Wosnick, J. H.; Shoichet, M. S. *Chem. Mater.* **2008**, *20*, 55–60. (e) DeForest, C. A.; Polizzotti, B. D.; Anseth, K. S. *Nat. Mater.* **2009**, *8*, 659–664. (f) Lee, S.-H.; Moon, J. J.; West, J. L. *Biomaterials* **2008**, *29*, 2962–2968. (g) Khetan, S.; Katz, J. S.; Burdick, J. A. *Soft Matter* **2009**, *5*, 1601–1606. (h) Kloxin, A. M.; Kasko, A. M.; Salinas, C. N.; Anseth, K. S. *Science* **2009**, *324*, 59–63. (i) Katz, J. S.; Burdick, J. A. *Macromol. Biosci.* **2010**, *10*, 339–348. (j) Nichol, J. W.; Koshy, S. T.; Bae, H.; Hwang, C. M.; Yamanlar, S.; Khademhosseini, A. *Biomaterials* **2010**, *31*, 5536–5544. (k) Wylie, R. G.; Ahsan, S.; Aizawa, Y.; Maxwell, K. L.; Morshead, C. M.; Shoichet, M. S. *Nat. Mater.* **2011**, *10*, 799–806. (l) Mosiewicz, K. A.; Kolb, L.; van der Vlies, A. J.; Martino, M. M.; Lienemann, P. S.; Hubbell, J. A.; Ehrbar, M.; Lutolf, M. P. *Nat. Mater.* **2013**, *12*, 1072–1078. (m) Yanagawa, F.; Sugiura, S.; Takagi, T.; Sumaru, K.; Camci-Unal, G.; Patel, A.; Khademhosseini, A.; Kanamori, T. *Adv. Healthcare Mater.* **2015**, *4*, 246–254. (n) Tsang, K. M. C.; Annabi, N.; Ercole, F.; Zhou, K.; Karst, D. J.; Li, F.; Haynes, J. M.; Evans, R. A.; Thissen, H.; Khademhosseini, A.; Forsythe, J. S. *Adv. Funct. Mater.* **2015**, *25*, 977–986.
- (8) (a) Frkanec, L.; Jokić, M.; Makarević, J.; Wolsperger, K.; Žinić, M. *J. Am. Chem. Soc.* **2002**, *124*, 9716–9717. (b) Matsumoto, S.; Yamaguchi, S.; Ueno, S.; Komatsu, H.; Ikeda, M.; Ishizuka, K.; Iko, Y.; Tabata, K. V.; Aoki, H.; Ito, S.; Noji, H.; Hamachi, I. *Chem. - Eur. J.* **2008**, *14*, 3977–3986. (c) Komatsu, H.; Matsumoto, S.; Tamaru, S. I.; Kaneko, K.; Ikeda, M.; Hamachi, I. *J. Am. Chem. Soc.* **2009**, *131*, 5580–5585. (d) He, M.; Li, J.; Tan, S.; Wang, R.; Zhang, Y. *J. Am. Chem. Soc.* **2013**, *135*, 18718–18721.
- (9) (a) Raeburn, J.; McDonald, T. O.; Adams, D. J. *Chem. Commun.* **2012**, 48, 9355–9357. (b) Maity, C.; Hendriksen, W. E.; vanEsch, J. H.; Eelkema, R. *Angew. Chem., Int. Ed.* **2015**, *54*, 998–1001.
- (10) Raeburn, J.; Alston, B.; Kroeger, J.; McDonald, T. O.; Howse, J. R.; Cameron, P. J.; Adams, D. J. *Mater. Horiz.* **2014**, *1*, 241–246.
- (11) Draper, E. R.; Eden, E. G. B.; McDonald, T. O.; Adams, D. J. *Nat. Chem.* **2015**, *7*, 848–852.
- (12) Okesola, B. O.; Vieira, V. M. P.; Cornwell, D. J.; Whitelaw, N. K.; Smith, D. K. *Soft Matter* **2015**, *11*, 4768–4787.
- (13) Cornwell, D. J.; Okesola, B. O.; Smith, D. K. *Soft Matter* **2013**, *9*, 8730–8736.
- (14) (a) Okesola, B. O.; Smith, D. K. *Chem. Commun.* **2013**, 49, 11164–11166. (b) Howe, E. J.; Okesola, B. O.; Smith, D. K. *Chem. Commun.* **2015**, *51*, 7451–7454.
- (15) (a) Zhang, Y.; Gu, H.; Yang, Z.; Xu, B. *J. Am. Chem. Soc.* **2003**, *125*, 13680–13681. (b) Jayawarna, V.; Ali, M.; Jowitt, T. A.; Miller, A. F.; Saiani, A.; Gough, J. E.; Ulijn, R. V. *Adv. Mater.* **2006**, *18*, 611–614. (c) Adams, D. J.; Butler, M. F.; Frith, W. J.; Kirkland, M.; Mullen, L.;

Sanderson, P. *Soft Matter* **2009**, *5*, 1856–1862. (d) Adams, D. J.; Mullen, L. M.; Berta, M.; Chen, L.; Frith, W. J. *Soft Matter* **2010**, *6*, 1971–1980. (e) Chen, L.; Revel, S.; Morris, K.; Serpell, L. C.; Adams, D. J. *Langmuir* **2010**, *26*, 13466–13471.

(16) Nebot, V. J.; Smith, D. K. In *Functional Molecular Gels*; Escuder, B., Miravet, J. F., Eds.; Royal Society of Chemistry: Cambridge, UK, 2014; pp 30–66.

(17) (a) Avrami, M. *J. Chem. Phys.* **1939**, *7*, 1103–1122. (b) Avrami, M. *J. Chem. Phys.* **1940**, *8*, 212–224. (c) Avrami, M. *J. Chem. Phys.* **1941**, *9*, 177–184.

(18) Huang, X.; Terech, P.; Raghavan, S. R.; Weiss, R. G. *J. Am. Chem. Soc.* **2005**, *127*, 4336–4344.

(19) Raeburn, J.; Pont, G.; Chen, L.; Cesbron, Y.; Lévy, R.; Adams, D. J. *Soft Matter* **2012**, *8*, 1168–1174.

(20) (a) Rodríguez-Llansola, F.; Escuder, B.; Miravet, J. F. *J. Am. Chem. Soc.* **2009**, *131*, 11478–11484. (b) Tang, C.; Smith, A. M.; Collins, R. F.; Ulijn, R. V.; Saiani, A. *Langmuir* **2009**, *25*, 9447–9453. (c) Chen, L.; Morris, K.; Laybourn, A.; Elias, D.; Hicks, M. R.; Rodger, A.; Serpell, L.; Adams, D. J. *Langmuir* **2010**, *26*, 5232–5242. (d) Reddy, A.; Sharma, A.; Srivastava, A. *Chem. - Eur. J.* **2012**, *18*, 7575–7581. (e) Wallace, M.; Iggo, J. A.; Adams, D. J. *Soft Matter* **2015**, *11*, 7739–7747.

(21) For a review see: (a) Cornwell, D. J.; Smith, D. K. *Mater. Horiz.* **2015**, *2*, 279–293. For examples see: (b) Chen, L.; Revel, S.; Morris, K.; Spiller, D. G.; Serpell, L. C.; Adams, D. J. *Chem. Commun.* **2010**, *46*, 6738–6740. (c) Pont, G.; Chen, L.; Spiller, D. G.; Adams, D. J. *Soft Matter* **2012**, *8*, 7797–7802.

(22) Cardoso, A. Z.; Alvarez, A. E. A.; Cattoz, B. N.; Griffiths, P. C.; King, S. M.; Frith, W. J.; Adams, D. J. *Faraday Discuss.* **2013**, *166*, 101–116.

(23) Draper, E. R.; Mears, L. L. E.; Castilla, A. M.; King, S. M.; McDonald, T. O.; Akhtar, R.; Adams, D. J. *RSC Adv.* **2015**, *5*, 95369–95378.

(24) Selimović, Š.; Oh, J.; Bae, H.; Dokmeci, M.; Khademhosseini, A. *Polymers* **2012**, *4*, 1554–1579.